KINETICS OF COMBUSTION IN THE LAYERED Ni–Al SYSTEM

V. A. Shcherbakov[1], A. S. Shteinberg[2]*, and Z. A. Munir[3]

[1]Institute of Structural Macrokinetics and Materials Science,
Russian Academy of Sciences, Chernogolovka, 142432 Russia
[2]Semenov Institute of Chemical Physics, Russian Academy of Sciences, Kosygin St., 4,
Moscow, 117977, Russia
[3]Facility for Advanced Combustion Synthesis, Department of Chemical Engineering and
Materials Science, University of California, Davis, California, 95616, USA

Abstract

Theoretical analysis and experimental results on the combustion in the Ni–Al layered system are presented. Combustion wave temperature and velocity were measured and microstructural and compositional determinations were made. The latter were made on products of complete combustion and on quenched samples using metallographic and electron microprobe analyses. The dependence of temperature in the reaction zone on the degree of conversion was calculated from equations of chemical kinetics and heat balance. The reaction was found to involve two stages: one proceeding in the liquid phase and the other in the solid phase. The former determines the combustion velocity, while the latter determines the adiabatic combustion temperature. The rate of heat release in the bulk and the combustion velocity were calculated with the assumption that the reaction is controlled by the dissolution of solid Ni in liquid Al. The experimental results are in good agreement with theoretical predictions.

Key words: SHS, combustion synthesis, gasless combustion, intermetallides, NiAl.

---

* To whom correspondence should be addressed. E-mail: shteinberg@aol.com
Present address: 61, Fairlawn Dr., Berkeley, CA 94708, USA. Tel/Fax (510)649-8203

1. Introduction

The theory of gasless combustion was largely developed for a model sample consisting of alternating planar layers of reactants [Aldushin and Khaikin, 1974; Hardt and Fung, 1973; Khaikin, 1975 and 1977]. However, the theory has only been validated by direct experimental observations in a very limited number of recent investigations. In general, experimental data presented in the literature were largely obtained by using samples compacted from mixtures of metals and nonmetals powders. A quantitative comparison between theoretical predictions and experimental results is difficult due to absence of data on the kinetics of high-temperature reactions and parameters of mass and heat transfer. The difficulties are caused primarily by the changes in the reaction interface (heterogeneity scale) because of different processes taking place in the combustion wave. These include melting, capillary spreading [Shkiro and Borovinskaya, 1975, Nekrasov *et al.*, 1978], dissolution of the refractory particles in the melted reagent [Shteinberg and Knyazik, 1994], reduction of particle size of the refractory reactant [Shcherbakov, 1996], etc.

Model layered systems provide a near-ideal geometry for experimental studies of the kinetic processes of product formation in gasless combustion. For a system with planar reaction interfaces, the thermal characteristics of the sample can be determined with a reasonably good accuracy and the reaction interface in a layered sample remains unchanged during combustion. These considerations make it possible to compare the experimental results with the theoretical predictions on a quantitative basis.

Combustion in bimetallic samples was investigated earlier on metallic wires coated with another metal [Vadchenko *et al*., 1987]. The disadvantage of this method for investigating the combustion mechanism is the dramatic change in the geometry caused by melting and the formation of separate drops. A high degree of conversion (approaching 100%) cannot be attained in such experiments due to the burning out of the wire because of local overheating. These problems can be solved by using a multilayered samples consisting of a set of Ni and Al foils [Anselmi-Tamburini and Munir, 1989]. The starting layered 2 mm thick sample was placed into a "chemical oven" composed of a compacted mixture of Ni and Al powders. Combustion in the

chemical oven, propagating in the form of a wave, ignited combustion in the imbedded multilayered sample. The combustion velocity for samples made with Ni (12.5 μm thick) and Al (19 μm thick) layers was found to be in the range of 10–12 $cm.s^{-1}$. However, application of the chemical oven as an igniter for measuring combustion velocities in samples of different compositions is not always suitable for quantitative analysis. Ignition of the sample during combustion in the chemical oven does not allow one to distinguish the conventional combustion mode from the mode of control. In the former case, combustion velocity does not depend on the nature of the igniter, while in the latter one, combustion velocity is determined by the velocity of motion of the igniting hot spot along the lateral face of the sample (velocity of combustion in the chemical oven).

Direct combustion in multilayered samples (Ni and Al layers 10–20 nm thick) was also studied [Ma *et al*., 1990]. The velocity of combustion initiated by an electric spark was found to be 4 $m.s^{-1}$. Recently combustion in Ni–Al systems was also investigated using free-standing multilayer samples which had been formed in ultrahigh vacuum by electron beam evaporation or by sputtering [Dyer *et al*., 1994; Dyer and Munir, 1995; Weihs, 1997]. For the case of the Ni:Al stoichiometry of 1:1, the Al layer thickness was varied in the approximate range 200–500 nm. Such multilayer systems combusted with corresponding velocities in the approximate range of 200 to 60 $cm.s^{-1}$. Multilayer systems with a Ni:Al stoichoimetry of 3:1 had lower velocites and showed a dependence on thickness of the Al and the Ni layers. The dependence of the wave velocity on layer thickness was found to be in qualitative agreement with theoretical predictions developed in the works of [Hardt and Phung, 1973; Armstrong and Koszykowski, 1990.] Record high rates of gasless combustion in multilayer systems were obtained in a series of studies by Weihs [Weihs, 1997]. However, experimentally validated research on the mechanism of gasless combustion and phase formation in systems with a melting reagent is far from completion. It has been assumed in previous theoretical studies that phase transition (the melting of one of the reagents) has only a negative effect on the rate of combustion front propagation [Aldushin and Merzhanov, 1978]. However, macrokinetic and kinetic research by Shteinberg and co-authors, based on Electrothermal Explosion method [Knyazik et al., 1985, Knyazik and Shteinberg, 1990; Shteinberg and Knyazik, 1992; Shteinberg and Knyazik, 1994] demonstrates that the melting and liquid-phase dissolution result in the intensification of the interaction process, even when the

effect of capillary spreading is not accounted for. These works demonstrated for the fir st time that the rate of propagation of the gasless combustion front in systems of the type Ti+C, Ni+Al, etc. is determined by the intensity of dissolution of one (solid) component in the liquid phase (melted phase) of another component. Perhaps this contradiction is responsible for the absence of a precise mathematical model for the rate of front propagation, a model that would describe adequately the principal macrokinetic dependencies of the combustion process on melting in the preheat region.

Therefore, the goal of the work described in this paper was to study quantitatively the macrokinetics of heat release in the front of gasless combustion in the layered Ni-Al system. One of the objectives was to determine the effect of the refractory reagent dissolution process, never studied before, on the laws of combustion and phase formation.

2. Experimental

A schematic of the experiment multilayer ensemble is shown in Figure 1. The samples were prepared by alternately winding 50 μm thick Ni (1) and Al (2) foils tightly onto a mandrel rod (5 mm in diameter). The Ni foil was of the NP-2 brand (99.9% pure) while Al foil, of the A3 brand (99.9% pure). After the removal of the mandrel, the resulting sample (15 mm in outer diameter, 60 mm in length, with 100 layers of each metal) was covered with mica (4) and then a nichrome wire (3) was wound around it. Combustion was initiated by electrically heating the nichrome wire. The temperature of the sample was uniform along its length prior to ignition, a circumstance resulting from the low rate of preheating (50^{o}C/min) and the high thermal conductivity of the sample. After ignition, the nichrome wire was deactivated. The wave that resulted was self-sustaining. The temperature of the sample during the preheat and wave propagation stages was measured by 100 μm diameter chromel-alumel thermocouples (5), placed at two locations as shown in Figure 1. After amplification (6) the signals from the thermocouples were sent to a recording oscilloscope (7). The product was analyzed for elemental distribution by electron-probe microanalysis (JCXA-733 apparatus) and the microstructure was evaluated metallographically.

3. Experimental Results

3.1. *Combustion Wave Parameters*:

A typical temperature profile of the combustion wave in the layered sample is shown in Figure 2 (curve 1). The observed steady-state wave propagation occurred at an initial (preheating) temperature of 540°C. At this temperature the sample is on the verge of combustion, but a wave does not propagate. Figure 2 also shows the specific rate of heat release during the reaction (curve 2). The reactants in the wave region are solid Ni and liquid Al as judged by the fact that the maximum combustion temperature is 1100°C. This value is between the melting points of Al and Ni, 660 and 1453°C, respectively. The mean combustion velocity calculated from the temporal position of the two thermocouple signals was 3.7 $mm.s^{-1}$. The inflection point in the temperature profile separates the preheating zone from the reaction zone. This point corresponds to a temperature of 640°C, which is the eutectic temperature of the $NiAl_3$–Al binary. Heat evolution during the reaction of Ni with Al starts at this temperature [Gasparyan and Shteinberg, 1988].

3.2. *Morphology of Combustion Products*:

The Ni and Al concentration profiles obtained from an electron microprobe analysis[1)] for the products of combustion are presented in Figure 3. The maximum levels of Al in the Ni layer and Ni in the Al layer are 5 and 64 wt %, respectively. By comparing the experimental results with the Ni-Al phase diagram it is possible to identify the combustion products in the two layers as a solid solution of Al in Ni in the Ni layer and Ni_2Al_3 in the Al layer. The microstructure of the product[2)] is presented in Figure 4. During combustion, the thickness of the Ni layers decreased from 50 to 20 μm while the thickness of all the nickel aluminide layers increased up to 100 μm. The increase in the thickness of aluminide layers is caused by Ni dissolution as well as by the filling of gaps between the Ni and Al layers with molten Al, giving rise to the formation of aluminide layer of higher thickness.

[1)] The electron microprobe analysis was made by Dr. Yu. A. Gal'chenko.

[2)] The metallographic analyses of the final product were made by Drs. G. A. Vishnyakova and A. N. Belikova.

The expansion of Al (≈13 vol % [Hatch, 1989]) upon melting results not only in filling the gas gaps between layers of the foils but also leads to another interesting phenomenon. Due to high hydrodynamic pressure (a result of the melting of Al in a closed volume), the liquid phase flows along the sample axis toward the combustion products. Drops of Al spraying from the combusted part of the sample were seen in the recorded frames of the combustion process. This results in a decrease in the aluminum content of the product, relative to the initial composition.

Selected results on the phase composition of the product as related to the thickness of the molten Al layer are presented in Table 1. The content of the dissolved Ni in the aluminide decreases with an increase in the thickness of the Al layer, δ_1. The phases of nickel aluminide were found to form as follows: at δ_1=30 μm, NiAl occupies the central part of the sample while Ni_3Al is adjacent to the Ni layer (Fig. 4 (a)). With an increase in δ_1 (to 50 μm), Ni_2Al_3 and NiAl form in the aluminide layer (Fig. 4(b)). A single-phase product (Ni_2Al_3) forms at δ_1=85 μm. At δ_1=100 μm, Ni_2Al_3 and $NiAl_3$ occupy the central part while Ni_2Al_3 occupies the areas adjacent to the Ni layer (Fig. 4 (c)). In order to freeze the combustion front, samples were quenched in water after the initiation of the wave. The microstructure of the quenched products is shown in Fig. 4 (d). The aluminide layer consists of the eutectic mixture of Al and $NiAl_3$. The microstructure of the eutectic phase provides information on phase formation during crystallization from the melt. In Figure 4 (d) the Ni layer is separated from the melt by a thin (about 1 μm) Ni_2Al_3 layer. The latter is believed to have formed by liquid Al diffusion in solid Ni. The diffusion of atoms of a molten phase into a solid and the subsequent formation of solid solutions or compounds (at a given temperature) is followed by dissolution into the liquid phase [Savitskii, 1991]. The degree of conversion in Ni and Al layers is markedly different: the diffusion flux from solid Ni into liquid Al determined by the partial diffusion coefficients of the components is predominant [Itin and Naiborodenko, 1977]. In the initial stage, the aluminide layer grows towards Ni because the aluminide dissolves in the melt in the opposite side. The liquid-phase stage represents the dissolution of solid Ni in liquid Al.

4. Discussion

4.1. Formation of Combustion Products

4.1.1. *Reaction Route*:

The reaction route (i.e., temperature profile in the reaction zone vs. degree of conversion) must be identified in order to determine the mechanism of product formation. Propagation of the combustion wave in a condensed medium can be described by the following equations for chemical kinetics and heat balance [Merzhanov and Khaikin, 1988]:

$$u\frac{dh}{dx} = k_0 j\,(h)\exp(-E/RT\,) \tag{1}$$

$$a\frac{d^2T}{dx^2} - u\frac{dT}{dx} + \frac{Q}{c}k_0 j\,(h)\exp(-E/RT) = 0 \tag{2}$$

$$x = -\infty: \qquad T = T_0 \qquad\qquad x = +\infty: \qquad T = T_b \tag{3}$$

where u is the combustion velocity; a is the thermal diffusivity; $\varphi(\eta)$ is the kinetic function; Q is the enthalpy of the reaction; k_o is the reaction rate constant; c is the heat capacity; E is the activation energy; R is the universal gas constant; T is temperature; T_0 is the initial temperature; T_b is the adiabatic combustion temperature; and x is the coordinate.

Dissolution is a low activated process described by the equation of first-order reaction. At $E = 0$ and $\varphi(h) = 1 - h$, we have

$$u\frac{dh}{dx} = k_0(1-h) \tag{4}$$

$$a\frac{d^2T}{dx^2} - u\frac{dT}{dx} + \frac{Q}{c}k_0(1-h) = 0 \tag{5}$$

By integrating Eq (4), we obtain the conversion degree as a function of coordinate:

$$h = 1 - \exp(-k_0 x/u) \tag{6}$$

Substituting Eq (6) into Eq (5), we obtain

$$a\frac{d^2T}{dx^2} - u\frac{dT}{dx} + \frac{Q}{c}k_0\exp(-k_0 x/u) = 0 \tag{7}$$

The solution for Eq (7) with boundary conditions given in Eq (3) has the following form:

$$T = T_b - \frac{Q(1-h)}{c(1+k_0 a/u^2)} \tag{8}$$

However, determination of the reaction route is difficult due to absence of data on the combustion velocity and the reaction rate constant. The temperature rise is a linear function of the degree of conversion. In this case, only the initial and final reaction temperatures are to be measured. For combustion in a liquid phase, the reaction starts at the melting point of the low-melting reactant. The maximum combustion temperature can be calculated as [Aldushin and Merzhanov, 1978; Merzhanov and Khaikin, 1988]

$$T_b = T_0 + (Q\text{-}L)/c \tag{9}$$

4.1.2. ***Mechanism of Products Formation****:*

Calculated temperature rise vs. fraction of dissolved Ni (conversion degree) is plotted on the Ni–Al phase diagram [Singleton *et al.*, 1990], Figure 5. For $T_0 < 400^oC$, the curves for the temperature rise intercept the liquidus line at T_{cr}. The intercept separates the area of reaction in a liquid phase from that of reaction in the solid phase. For the former case, the reaction product is dissolved Ni in molten Al and for the latter, the product is a layer of solid nickel aluminide. The liquid stage of the reaction is complete at the temperature of saturated melt formation while the solid one is at the adiabatic combustion temperature.

The concentration of the saturated melt can be calculated from the intercept of the temperature rise curves and the liquidus line. For low concentrations of the saturated melt, the lower nickel aluminides ($NiAl_3$ and Ni_2Al_3) transform subsequently into the higher nickel aluminides (Ni_3Al and NiAl). The maximum grain size of nickel aluminides was found to correspond to half of the product layer thickness (see Figure 4 (c)).

The melt temperature does not depend on the initial temperature, as does the adiabatic temperature. Thus the slope of a temperature rise curve is a function of the initial temperature. As the latter increases, the intercept point and conversion degree attained during the liquid-phase stage also increase. For $T_0 > 400^oC$, the curves do not intercept the liquidus, as seen in Figure 5.

In this case, the reaction proceeds only in the liquid phase. The higher aluminides crystallize from the melt without an intermediate stage in which lower aluminides form. The size of the product grains depends on the crystallization rate.

Duration of the reaction in the liquid (t_L) and solid (t_S) phases depends on the time it takes for the solid component to dissolve in the Al layer, i.e.,

$$t = \frac{\ddot{a}^2}{D} \tag{10}$$

In the calculations, we used diffusion coefficients for Ni into solid and liquid Al [Eremenko *et al*., 1975]. Formation of the product was found to be limited by Ni diffusion through the solid product layer (Table 1): thin melt layers contain the higher aluminides (Ni_3Al and NiAl) while the thick ones contain the lower aluminides ($NiAl_3$ and Ni_2Al_3). This confirms that at T_{cr} (formation of the saturated melt), the reaction between Ni and Al does not stop but decelerates. At adiabatic conditions, the reaction proceeds until the reactants are consumed and equilibrium is attained.

We now consider the experiments carried out by Alexandrov and by Holt and co-workers [Boldyrev *et al*., 1981; Holt *et al*., 1990] using synchrotron radiation. A marked delay in product formation was observed during combustion in Ni–Al pellets. Formation of the NiAl phase took place 70 seconds after the passage of the combustion front. The authors could not identify the intermediate phases detected during the process. The delay is caused by the dependence of the combustion velocity on the formation of the product melt. Structure formation in the product proceeds during the second stage of the process. In the initial stage, identification of the combustion products by time-resolved X-ray diffraction may be rather difficult due to the highly imperfect nature of the structure of nickel aluminide.

It is need to note that in Alexandrov's and Rogachev's [Rogachev et al, 1994] experiments on combustion in the Ni–Al system have observed formation first phase NiAl and not phases $NiAl_3$ or Ni_2Al_3. The mechanism of product formation proposed allows give a simple explanation. The reason is to be that at first stage of interaction the reaction product is melt. Wherefore it can not determinate and study by X-Ray analysis, because it has not a crystal structure. The solid reaction product forms only at the second stage, when formed a saturated solution. According the Ni–Al

phase diagram from this saturated solution may be crystallized phase NiAl only.

4.2 Kinetics of Combustion

4.2.1. *Rate of Heat Release*.

In order to calculate the combustion velocity, the rate of heat release and the location of its source should be determined. The reaction does not perceptively proceed in the heat-up zone due to thermally activated diffusion in the solid Ni – solid Al system [Gertsiken *et al*., 1960]. Thermal diffusivity for the layered sample can be readily calculated from the thermal profile for the heat-up zone. The temperature profile can be described as follows:

$$T = T_0 + (T_m - T_0)\exp(-Ux/a) \tag{11}$$

The experimental curve (profile for the heat-up zone) is readily linearized in the semilogarithmic coordinates of Figure 6. The slope gives the thermal diffusivity (a_m) for the layered sample, i.e.,

$$a_m = u / tg\alpha_1 \approx 0.37 \text{ cm}^2/\text{s} \tag{12}$$

We now compare a_m and the calculated one (a_c). The lengthwise thermal diffusivity is calculated as

$$a = \frac{l_1 + l_2 x}{c_1 r_1 + c_2 r_2 x} \tag{13}$$

where ρ_1, c_1, λ_1 are, respectively, the density, heat capacity, and thermal conductivity of Al; ρ_2, c_2, λ_2 are, respectively, the density, heat capacity, and thermal conductivity of Ni; and $\xi=\delta_2/\delta_1$, is the stoichiometric coefficient[3)]. Substituting the data from Table 2 [Samsonov *et al*., 1965] into Eq (13), we obtain $a_c \approx 0.41 \text{cm}^2/\text{s}$. The good agreement between a_m and a_c confirms that the reaction does not proceed in the heat-up zone. By using the experimental data, we can calculate the rate of heat evolution by well known Zenin's metod [Zenin *et al*., 1980, Zenin 1990]

$$q_m = c r u \frac{dT}{dx} - l \frac{d^2T}{dx^2} \tag{14}$$

where

[3)] For Ni/Al=1/1 (mole ratio), $\xi = 0.64$.

$$c = \frac{c_1 r_1 + c_2 r_2 x}{r_1 + r_2 x} \tag{15}$$

$$r = \frac{r_1 + r_2 x}{1 + x} \tag{16}$$

$$l = \frac{l_1 + l_2 x}{1 + x} \tag{17}$$

The derivatives of temperature were determined from the temperature profile of the combustion wave. The rate of heat release as a function of time is shown in Figure 2 (curve 2). For $T > 640^{o}$C, q_{m} increases sharply, attaining a value of ≈360 W/cm^3 (its maximum value) at the melting point of aluminum. With further increase in temperature, the rate of heat release decreases.

We now calculate the rate of heat release per volume assuming the reaction is limited by the rate of the dissolution of solid Ni into liquid Al [Frank-Kamenetskii, 1987]:

$$q_c = \frac{2 j Q}{\ddot{a}_1 (1 + \hat{\imath})} \tag{18}$$

where Q is the enthalpy for Ni dissolution in liquid Al; j is the diffusion flux, which is defined by

$$j = \frac{2 \Delta m \; r \; D_L}{\ddot{a}_1} \tag{19}$$

with $\Delta m = m_{\text{S}} - m$; m_{S} is the Ni weight fraction in the saturated melt; m is the weight fraction of dissolved Ni; and r is the melt density.

Substituting Eq (19) into Eq (18), we obtain,

$$q_c = \frac{4 \Delta m r \; Q \, D_L}{\ddot{a}_1^{\,2} (1 + \hat{\imath})} \tag{20}$$

At $\Delta m = m_{\text{s}}$, the heat release is maximum. For $D_{\text{L}} = 10^{-5}$ cm^2/s, Q = 1628 J/g, and Δm = 0.1 [Samsonov *et al.*, 1976; Eremenko *et al.*, 1975], q_{c} is about 400 W/cm^3. The small difference between q_{c} and q_{m} (≈10%) confirms the validity of the assumptions.

The rate of solid Ni dissolution in molten Al is proportional to Δm. The value of Δm can be calculated by using the dependence of the temperature of heat-up in the combustion wave on the degree of conversion at $T_0 = 540^{o}$C and $\xi = 1$ (Figure 5, curve 6). The theoretical Δm as a function

of T is presented in Figure 7 (curve 1). The eutectic is a saturated melt: at its melting point, Δm = 0. With an increase in temperature, Δm increases attaining its maximum value at the Al melting point. Further increase in temperature results in a decrease in Δm down to Δm = 0 (at T_{cr} the saturated melt forms). The slight deviation of $\Delta m(T)$ function from linearity at T=850^{o}C is caused by a preceding peritectic reaction. In Figure 7, the experimental functions $q = q(x)$ and $T = T(x)$ from Figure 2 in the form of a $q = q(t)$ diagram are presented. For the temperature interval between 670 and 1100°C, the rate of heat release quantitatively correlates with Δm. This confirm that the main heat release is caused by the dissolution of solid Ni into liquid Al.

4.2.2. ***Combustion Velocity***:

In case of a wide reaction zone, the combustion velocity is determined not by the maximum combustion temperature but by an intermediate one that can be referred to as a nominal boundary of the propagation and after burning zone [Khaikin, 1975; Shkiro and Borovinskaya, 1975]. This is connected with significant retardation (breaking) of heat release with increase in the conversion degree. The processes in the zone of after burning were theoretically proved [Aldushin *et al.*, 1972] not to have any marked effect on the combustion velocity.

Based on this, T_b is substituted for with T_{cr} in Eq (8). At h = 0 and $T = T_{mp}$ we have,

$$u_c^2 = k_0 a \left(\frac{T_{cr} - T_{mp}}{T_{mp} - T_0} \right) \tag{21}$$

The reaction constant can be calculated from the following formula

$$k_0 = \frac{q_c}{r\,Q} \tag{22}$$

Substituting Eq (22) into Eq (21), we can express the combustion velocity as

$$u_c^2 = \frac{a\,q_c}{r\,Q} \left(\frac{T_{cr} - T_{mp}}{T_{mp} - T_0} \right) \tag{23}$$

We now analyze the combustion velocity for the Ni–Al system as an experimental function of the initial temperature [Maslov *at al.,* 1976], by using Eq (23). For the sake of convenience, we consider the dimensionless function $y = u(T_0)/u(T_0^*)$, that is the ratio of combustion velocities at the initial temperature (T_0) to that at T_0^* = 20^{o}C. The formula for the calculated relative change in combustion velocity y_c is:

$$\text{ø}_c = \sqrt{\frac{(T_{cr} - T_{mp})}{(T_{cr}^{*} - T_{mp})} \frac{(T_{mp} - T_0^{*})}{(T_{mp} - T_0)}} \tag{24}$$

where T_{cr}^{*} is the temperature for the heat-up curve intercept with the liquidus line at $T_0^{*} = 20^{o}$C. The values of T_0, T_{cr}, experimental y_{exp}, and calculated y_c are given in Table 3. Note that y_{exp} and y_c are virtually identical. Note that y_{exp} and y_c are virtually identical. An increase in the combustion velocity by a factor of 2–3 with an increase in the initial temperature up to 300°C is caused by a weak dependence of the concentration of the saturated melt on temperature. As the initial temperature approaches T_{mp}, the combustion velocity increases markedly. This explains the high combustion velocities reported in the literature [Vadchenko *et al*., 1987; Anselmi-Tamburini and Munir, 1989].

The heterogeneity scale is an important parameter affecting gasless combustion velocity. Substituting Eq (16) into Eq (23), we obtain the combustion velocity as a function of Al layer thickness:

$$u_c^2 = \frac{4\, a\, \Delta m\, D_L}{\ddot{a}_1^{\,2}(1+\hat{\imath})} \left(\frac{T_{cr} - T_{mp}}{T_{mp} - T_0} \right) \tag{25}$$

And substituting the required values into Eq (25), we obtain $u_c \approx 0.4$ cm.s^{-1}. The values of u_c and u_m are in good agreement. Also, we found by numerical analysis that at $T_0 = 100$–400°C,

$$\frac{4\Delta m}{(1+\hat{\imath})} \left(\frac{T_{cr} - T_{mp}}{T_{mp} - T_0} \right) \approx 1 \tag{26}$$

This allows us to simplify the expression for the combustion velocity as

$$u_c = \frac{\sqrt{a\, D_L}}{\ddot{a}_1} \tag{27}$$

In accordance with Eq (27), the burning time for the heat-up layer ($t_1 = a/u^2$) is identical to the duration of the liquid-phase stage ($t_2 = \delta_1^{\,2}/D_L$).

During SHS reactions in Ni–Al pellets Al melts in the combustion wave and spreads onto the surface of Ni particles resulting in a marked change in the reaction surface. The thickness of Al layer (δ^{*}) after spreading on surface spherical Ni particle (d) can be calculated from the formula

$$\delta^* = 0.18d \tag{28}$$

where d is the mean diameter of Ni particles. The size of Ni and Al particles correspond the stoichiometry ratio.

The combustion velocity as a function of the Al layer thickness is presented in Figure 8. We used our experimental data as well as data from Maslov *et al.*, (1976); Lebrat *et al.*, (1992); Naiborodenko *et al.*, (1975); and Ma *et al.*, (1990). For δ>1 μm, the data can be easily linearized while for $\delta \approx 10$ nm the curve representing the combustion velocity as a function of Al layer thickness is far from linear. This may be explained by chemical reaction at low temperature (lower than the melting point of Al) on the stage of preparing the starting sample. In this case, the end product accumulates before the initiation of combustion, resulting in a decrease in the combustion velocity.

The diffusion coefficient determined from the slope (see the Figure 8) is

$$D = \frac{tg^2 \acute{a}_2}{a} \approx 10^{-5}, \text{ cm}^2.\text{s}^{-1} \tag{29}$$

The resulting diffusion coefficient is identical to that of Ni diffusion in molten Al [Eremenko *et al.*, 1975] and is in good agreement with the experimental data obtained by Electrothermal Explosion (ETE) [Shteinberg and Knyazik, 1994]. This confirms the dependence of the combustion velocity on the diffusion rate in the liquid phase.

5. Conclusions

1. We investigated the combustion of samples consisting of alternating Ni and Al layers. The combustion velocity and temperature were measured. The structure of combusted and quenched samples was evaluated by metallographic and microprobe analyses. Phase composition and maximum size of the monophase product grains were found to depend on the Al layer thickness.

2. The reaction route (temperature of heat-up as a function of conversion degree) was determined by using solutions of the chemical kinetics and heat balance equations. For a low-activated first-order reaction, the temperature of heat-up was found to be a linear function of conversion degree. The calculated heat-up curves plotted onto the phase diagram for the Ni–Al system were shown to intercept with the liquidus line. The intercept separated areas of the liquid-

phase stage of the reaction from that of the solid-phase stage. Duration of the former stage is determined by saturated melt formation while duration of the latter by growth of the solid product layer.

3. The rate of heat release per volume and the combustion velocity were calculated. The macrokinetics of the combustion process is limited by the rate of solid Ni dissolution in liquid Al. Theoretical calculations and experimental data are in good agreement.

Acknowledgments

This work was supported by the Russian Academy of Sciences (project no.47, July 13, 1998) and by the US National Science Foundation (ZAM).

We are grateful to Dr. E.N. Rumanov for his assistance in calculating the temperature of the conversion degree in the reaction zone.

References

Aldushin A. P., Martem'yanova, T. M., Merzhanov, A. G., Khaikin, B. I., and Shkadinskii, K. G., (1972). "Propagation of Front of an Exothermic Reaction in Condensed Mixtures with Interaction of Components Through a Layer of High-melting Product." *Combust. Expl. Shock Waves*, **8**(2), 159–167.

Aldushin, A. P., and Merzhanov, A. G. (1978). "Gasless combustion with phase transformation," *Dokl. Phys. Chem.*, **236,** 973.

Aldushin, A. P. and Khaikin, B. I., (1974). "Toward the Theory of Combustion of Mixed Systems Forming Condensed Reaction Products." *Fiz. Goreniya Vzryva*, **10**(3), 313–323.

Anselmi-Tamburini, U. and Munir, Z. A., (1989). "The Propagation of a Solid State Combustion Wave in Ni–Al Foils." *J. Appl. Phys.*, **66**(10), 5035–5039.

Armstrong, R. and Koszykowski, M., (1990). "Combustion Theory for Sandwiches of Alloyable Materials." In: *Combustion and Plasma Synthesis of High-Temperature Materials*, Z. A. Munir and J. B. Holt, Editors, VCH Publishers, NY, 88–99.

Boldyrev V. V., Aleksandrov, V. V., Korchagin, M. A., Tolochko, B. P., Gusenko, S. N., Sokolov, A. S., Sheromov, M. A., and Lyakhov, N. Z., (1981). "Study of Phase Formation Dynamics

at Nickel Monoaluminide Synthesis in Combustion Regime." *Dokl. Akad. Nauk SSSR*, **259**(5), 1127–1129.

Dyer, T. S., Munir, Z. A., and Ruth, V., (1994). "The Combustion Synthesis of Multilayer Ni–Al Systems." *Scripta Metall. et Mater*., **30**, 1281–1286.

Dyer, T. S. and Munir, Z. A., (1995). "The Synthesis of Nickel Aluminides from Multilayer Self-Prpopagating Combusion." *Metall. Trans. B,* **26**, 587–593.

Eremenko, V. N., Natanzon, Ya. V., Titov, V. P., and Tsydulko, A. G., (1975). "Kinetics of Dissolution of Nickel in Aluminum." *Izv. Akad. Nauk SSSR: Metally*, No. **1**, 64–66.

Frank-Kamenetskii, D. A., (1987). *Diffuziya i teploperedacha v khimicheskoi kinetike* (Diffusion and Heat Transfer in Chemical Kinetics). Moscow: Nauka.

Gasparyan, A. G. and Shteinberg, A. S., (1988). "Macrokinetics of Reaction and Thermal-Explosion in Ni and Al Powder Mixtures." *Combust. Expl. Shock Waves,* **24**(3), 324–330.

Gertsriken, S. D. and Dekhtyar, I. Ya., (1960). *Diffuziya v metallakh i splavakh v tvyordoi faze* (Diffusion in Metals and Alloys in Solid Phase). Moscow: Fizmatgiz.

Hardt, A. P. and Phung, P. V., (1973). "Propagation of Gasless Reaction in Solids." *Combust. Flame,* **21**(1), 77–89.

Hatch J. (ed.), (1984). *Aluminum: Properties and Physical Metallurgy*. American Society for Metals, Metals Park OH.

Holt, J. B., Wong, J., Larson, E., Waide, P., Rupp, B., and Frahm R., (1990). "A New Experimental Approach to Study Solid Combustion Reactions Using Synchrotron Radiation." In: *Proc. I American–Japanese Workshop on Combustion Synthesis*, 107–114.

Itin, V. I. and Naiborodenko, Yu. S., (1977). "Volume Changes for Nonisothermic Sintering and SHS of Porous Bodies." *Porosk. Metall.* (Kiev), **2**, 6–11.

Itin, V. I. and Naiborodenko, Yu. S., (1989). In: *Vysokotemperaturnii sintez intermetallicheskikh soedinenii* (High-Temperature Synthesis of Intermetallic Compounds). Tomsk: Izd. Tomsk. Univ., 211–214.

Knyazik, V. A., Merzhanov, A. G., Solomonov, V. B. and Shteinberg, A. S. "Macrokinetics of High-Temperature Titanium Interaction with Carbon under Electrothermal Explosion Conditions." In: *Comb. Explosion and Shock Waves*, vol. 21, No. 3, Nov. 1985, pp. 333-337. Original manuscript submitted April 27, 1983.

Knyazik, V. A. and Shteinberg, A. S., (1990).”Electrothermal Explosion in Heterogeneous Systems.” In: *Proceedings of the Joint Meeting of the Soviet and Italian Sections of the Combustion Institute*. Pisa, November 5-9, 1990. Napoli: Combust. Inst. Publ., 1990, 4.

Khaikin, B. I., (1977). "Combustion Zone Propagation in Systems Forming Condensed Reaction Products", *Proc. IV All-Union Symp. on Combustion and Explosion*, Moscow, 121–137.

Khaikin, B. I., (1975). “Toward the Theory of Combustion in Heterogeneous Condensed Media.” In: *Protsessy goreniya v khimicheskoi tekhnologii i metallurgii* (Combustion Processes in Chemical Technology and Metallurgy). Chernogolovka, 227–244.

Korchagin, M. A., Aleksandrov, V. V., and Gusenko, S. N., (1981). “Electron Microscopic Study of SHS-Systems Components Interaction.” In*: Problemy tekhnologicheskogo goreniya* (Problems of Technological Combustion), Chernogolovka, **1**, 14–16.

Lebrat J. P. and Varma A., (1992). “Self-Propagating High-Temperature Synthesis of Ni_3Al". *Combust. Sci. Technol.*, **88**, 211–221.

Ma, E., Thompson, C. V., Clevenger, L. A., and Tu, K. N., (1990). “Self-Propagating Explosive Reactions in Al/Ni Multilayer Thin Films.” *Appl. Phys. Lett*. **57**(12), 1262–1264.

Maslov, V. M., Borovinskaya, I. P., and Merzhanov, A. G., (1976). “Problem of Mechanism of Gasless Combustion.” *Combust. Expl. Shock Waves*, **12(**5), 631–637.

Merzhanov, A. G., Rumanov, E. N., and Khaikin B. I., (1972). “Multizone Combustion in Condensed Systems.” *Prikl. Mekh. Tekh. Fiz.* **6**, 99–105.

Merzhanov, A. G., (1990). “Self-Propagating High Temperature Synthesis: Twenty Years of Search and Findings.” In: *Combustion and Plasma Synthesis of High Temperature Materials*, Z. A. Munir and J. B. Holt, Editors, VCH Publishers, New York.

Merzhanov, A.G. and Khaikin B.I. **(**1988). “Theory of combustion waves in homogeneous media. “*Progr. Energy Combust. Sci.*, **14**, p.1–98.

Naiborodenko, Yu. S. and Itin, V. I., (1975). “Gasless Combustion of Metal-Powder Mixtures.” *Combust. Expl. Shock Waves,* **11**(3), 293–300.

Nekrasov, E.A., Maksimov Yu. M., Ziatdinov M. Kh. and Shteinberg A.S. (1978). “Capillary spreading influence on the combustion wave propagation in gasless systems.” *Combust. Expl. Shock Waves,* **14**(5), 26-33.

Philpot, K. A., Munir, Z. A., and Holt, J. B., (1987). “Investigation of the Synthesis of Nickel Aluminides Through Gasless Combustion.” *J. Mater. Sci*., **22**(1), 159–169.

Rogachev A.S. et al, Int. J. of SHS, **3**, (1994)

Rogachev A.S., Khomenko I.O., Varma A., Merzhanov A.G., Ponomarev V.I. **(**1994). "Mechanism of self-propagating high-temperature synthesis of nickel aluminides (Part 2): Crystal structure formation in a combustion wave." *Int. J. of SHS*, **3(**3), p.239–252.

Savitskii, A. P., (1991). *Zhidkofaznoe spekanie sistem s vzaimodeistvuyushchimi komponentami* (Liquid-Phase Sintering of Systems with Interacting Components). Nauka: Novosibirsk, 183p.

Samsonov, G. V., Burykina, A. L., and Goryachev, Yu. M., (1965). *Fiziko-khimicheskie svoistva elementov* (Physicochemical Properties of the Elements). Kiev: Naukova Dumka.

Samsonov, G. V.and Vinitskii, I. M., (1976). *Tugoplavkie soedineniya* (Refractory Compounds). Moscow: Metallurgiya.

Shcherbakov, A. V., (1996). "Diminution of Grain Size of Refractory Reagent in the Gasless Combustion Wave." *Dokl. Akad. Nauk*, **347**(5), 645–648.

Shcherbakov, V. A. and Sizov, A. N., (1996). "Porous Product Structure Formation at Combustion in Ti–C (Carbon Black) Mixture." *Dokl. Akad. Nauk*. **348**(1), 69–73.

Shkiro, V. M. and Borovinskaya, I. P., (1975). "Study of Combustion in Ti–C Systems." In: *Protsessy goreniya v khimicheskoi tekhnologii i metallurgii* (Combustion Processes in Chemical Technology and Metallurgy), Chernogolovka, 253–258.

Shteinberg, A. S. and Knyazik, V. A., (1992). "Macrokinetics of High-Temperature Heterogeneous Reactions: SHS Aspects." Pure and Appl. Chem., 64(7), 965-976.

Shteinberg, A. S. and Knyazik, V. A., (1994) "Electrocombustion." In: *Proc. Zel'dovich Memorial: Combustion, Detonation, Shock Waves.* Moscow, September 12–17, 358–372.

Sinel'nikova, V. S., Podergin, V. A., and Rechkin, V. N., (1965). *Alyuminidy* (Aluminides), Kiev: Naukova Dumka.

Singleton, M. F., Murray, J.L. and Nash P., (1990). "Al-Ni (Aluminium-Nickel)." In: *Binary Alloy Phase Diagrams*, T. B. Massalski, Editor, ASM International, NY, 181-183.

Vadchenko, S. G., Bulaev, A. M., Gal'chenko, Yu. A., and Merzhanov, A. G., (1987). "Interaction Mechanism in Laminar Bimetal Nickel-Titanium and Nickel-Aluminum Systems." *Combust. Expl. Shock Waves*, **23**(6), 706–715.

Weihs, T. P., (1997). "Self-Propagating Reactions in Multilayer Materials." In: *Handbook of Thin Film Process Technology*, F7, IOP Publishing, Ltd.

Zenin A.A., Merzhanov A.G., Nersisyan G.A. **(**1980). “The structure of the thermal wave in some SHS processes.” *Dokl. Akad. Nauk SSSR,* **250**(4), p.880–884.

Zenin A.A. (1990). “The thermal structure of solid flames.” *Pure Appl. Chem.,* **62**(5), p.889–8

Table 1. Composition of Combustion Product in Al Layer

Al layer thickness δ_1, μm	Composition of combustion products in Al Layer: in the central part	on the surface	Ni content, wt %	Reaction time, s t_L	t_S
20–35	NiAl	Ni_3Al	76–83	0.225	22.5
40–70	Ni_2Al_3	Ni_3Al; Ni_2Al_3	60–66	0.625	62.5
75–100	$NiAl_3$; Ni_2Al_3	Ni_2Al_3	53–57	2.5	250
50 (quenched)	Al(eutect.); $NiAl_3$	Ni_2Al_3	10–15	-	-

Table 2. Thermophysical Properties of Nickel and Aluminum

Metal	Thermal conductivity l, W/(cm K)	Heat capacity c, J/g K	Density r, g/cm^3	Thermal diffusivity a, cm^2/s
Al	2.35	1.0	2.7	0.84
Ni	0.62	0.5	8.9	0.18
Bimetal	1.5	0.62	5.8	0.42

Table 3. Effect of the Initial Temperature on Relative Change on the Combustion Velocity in the Ni–Al System

T_0, °C	u, cm.s^{-1}	T_{cr}, °C	ψ_{exp}	ψ_c
20	2.6	1300	1.00	1.00
100	3.0	1400	1.15	1.15
200	4.0	1480	1.54	1.33
250	4.7	1540	1.81	1.46
300	5.9	1600	2.27	1.62

Figure Captions:

1. Experimental setup: Ni foil (*1*); Al foil (*2*); nichrome spiral (*3*); mica (*4*); thermocouples (*5*); amplifier U7-1 (*6*); recording occilloscope N 117 (*7*).

2. Variation of temperature (1) and intensity of heat release (2) in combustion wave.

3. Ni (1) and Al (*2*) distribution through the layers.

4. Microstructure of the end (*a*, *b*, *c*) and quenched (*d*) combustion products. Nickel aluminide thickness (in mkm) is: 30 (*a*), 50 (*b*), 100 (*c*), 50 (*d*).

5. Phase diagram for the Ni–Al system and calculated warm-up temperature vs. conversion degree at $\xi = 0.64$ (stoichiometry composition) and the initial temperature 20 (*1*), 100 (*2*), 200 (*3*), 300 (*4*), 400^{o}C (*5*) and at $\xi = 1$ (nonstoichiometry experimental composition) and the initial temperature is 540^{o}C (*6*).

6. Towards the calculations based on temperature profile.

7. The theoretical Δm as a function of T (*1*) and experimental rate of heat release vs. temperature (*2*).

8. Combustion velocity vs. Al layer thickness.

■ - [Maslov *et al.,* 1976]; ● - [Naiborodentko *et al*., 1975];

○ - [Lebrat *et al*., 1992]; ▲ - [Ma *et al*., 1990];

△ - [Dyer *et al*., 1995]; ✱ - [Weihs *et al*., 1997].

□ - [Present study];

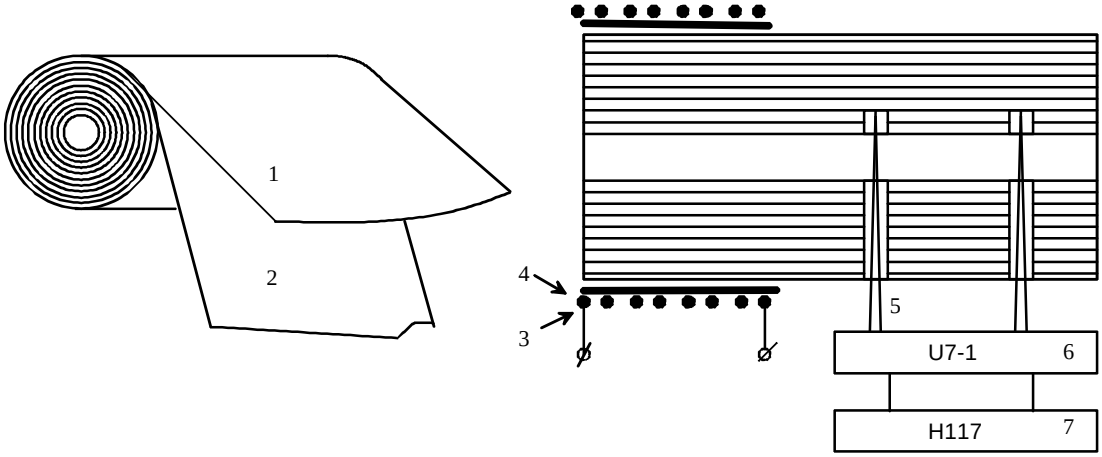

Fig.1. Experimental setup: Ni foil (1); Al foil (2); nichrome spiral (3); mica (4); thermocouples (5); amplifier U7-1 (6); recording occilloscope N 117 (7).

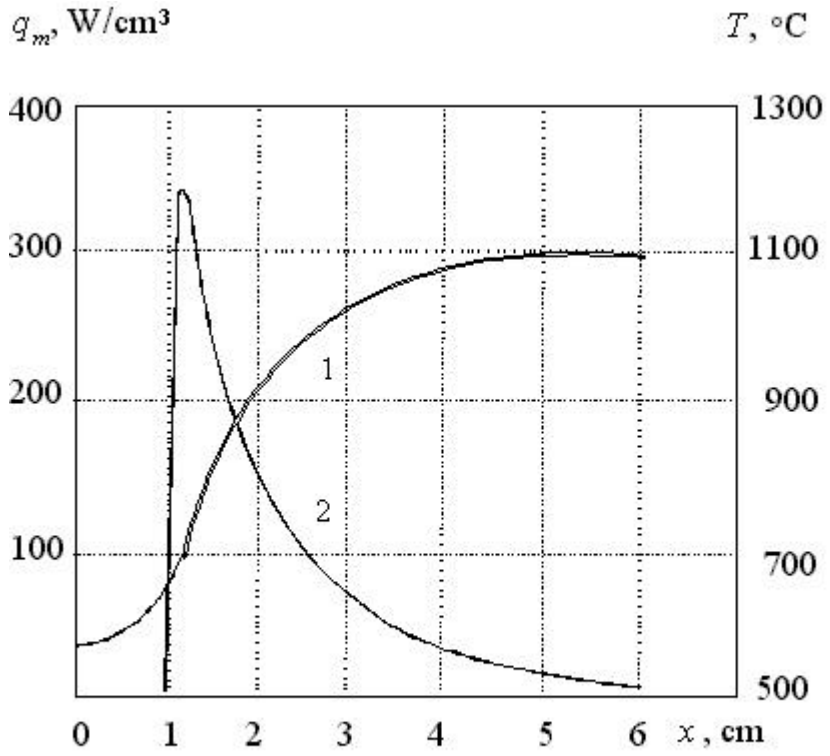

Fig. 2. Variation of temperature (1) and intensity of heat release (2) in combustion wave (*1*).

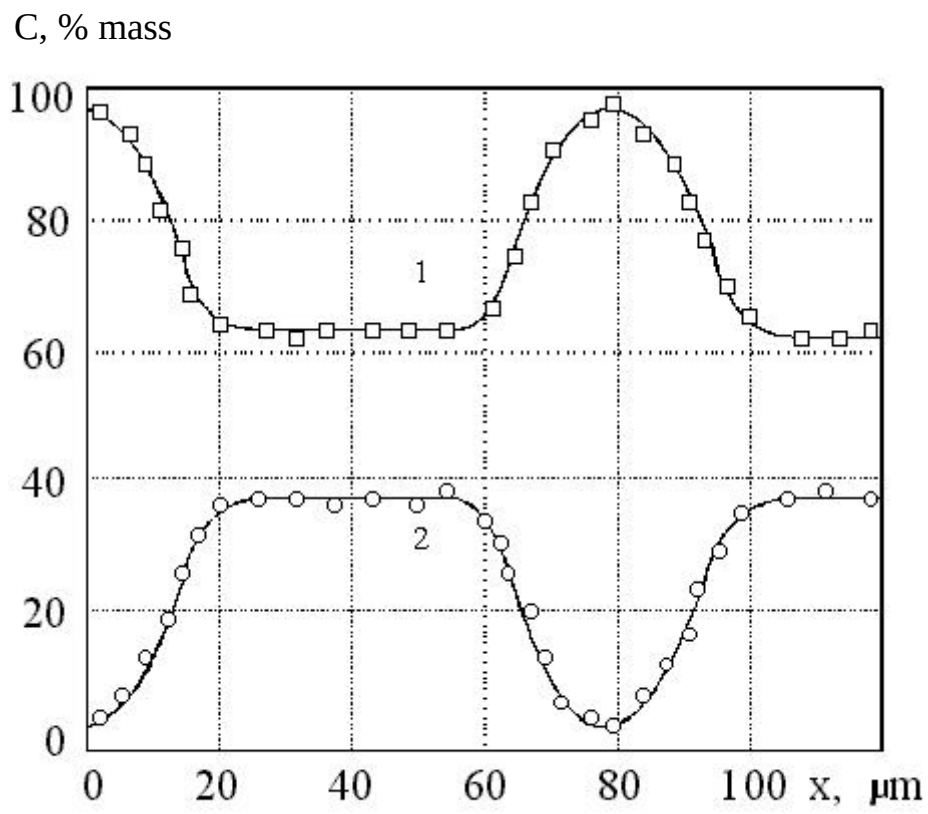

Fig. 3 Ni (1) and Al(2) distribution through the layers.

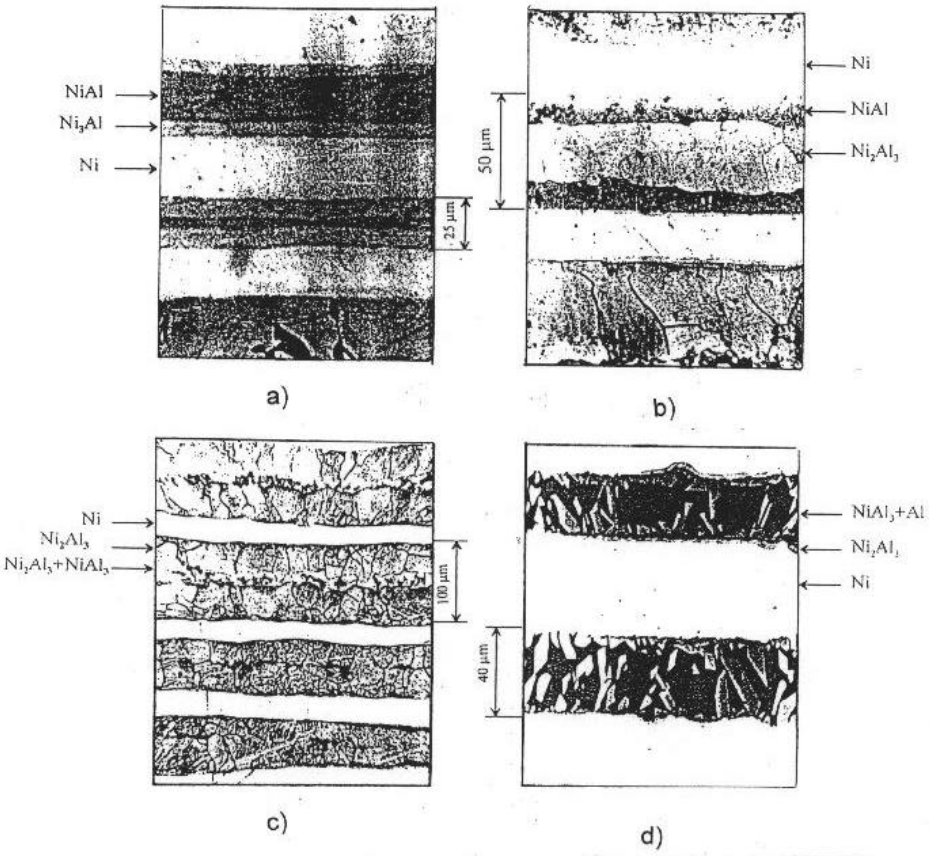

Fig. 4 Microstructure of end (a,b,c,) and quenched (d) combustion products. Nickel aluminide thickness (in mkm) is 30 (a), 50 (b), 100 (c) and 40 (d).

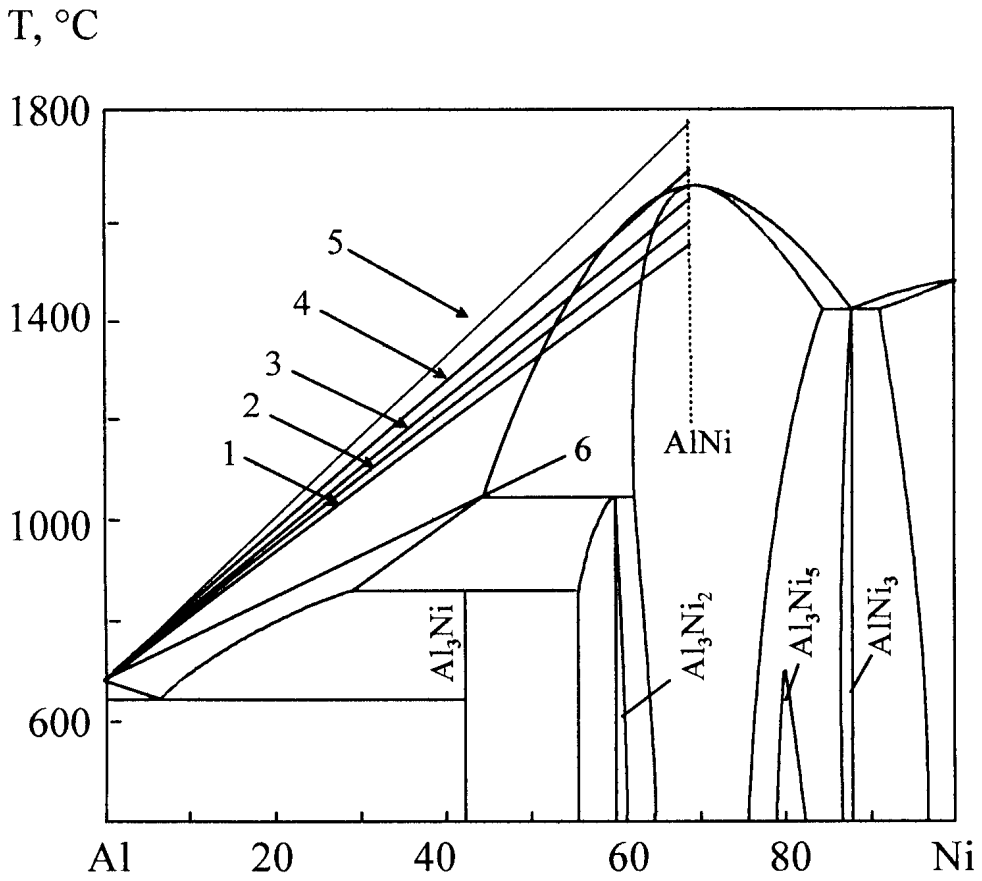

Fig. 5. Phase diagram for the Ni-Al system and calculated warm-up temperature vs. conversion degree at $\xi = 0.64$ and the initial temperature 20 (1), 100 (2), 200 (3), 300 (4), 400°C (5) and at $\xi = 1$ and the initial temperature is 540°C (6).

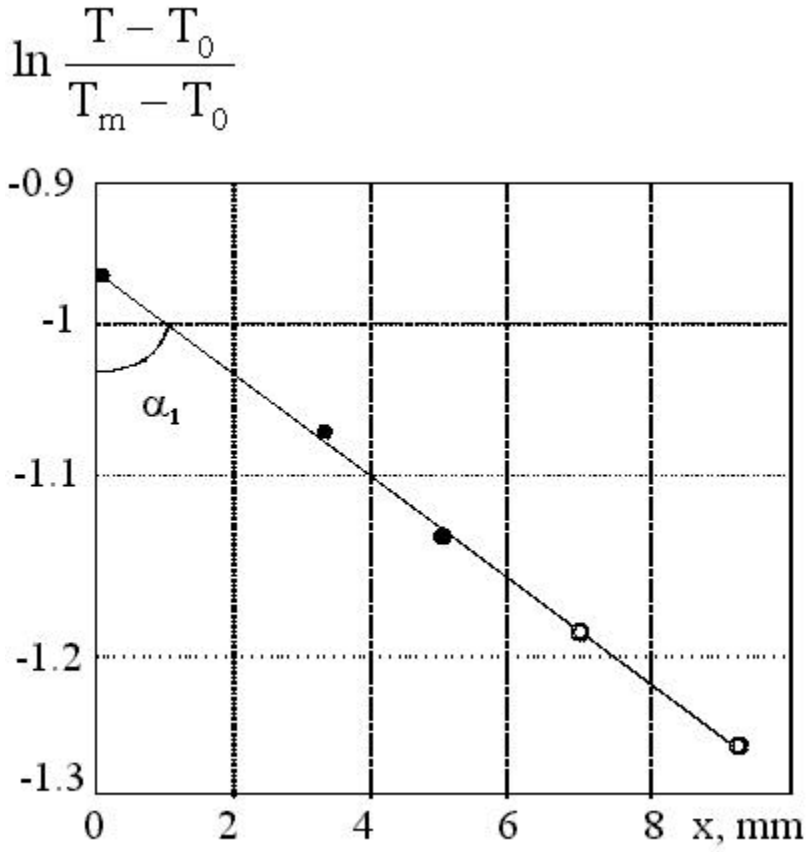

Fig. 6. Towards the calculations based on temperature profile.

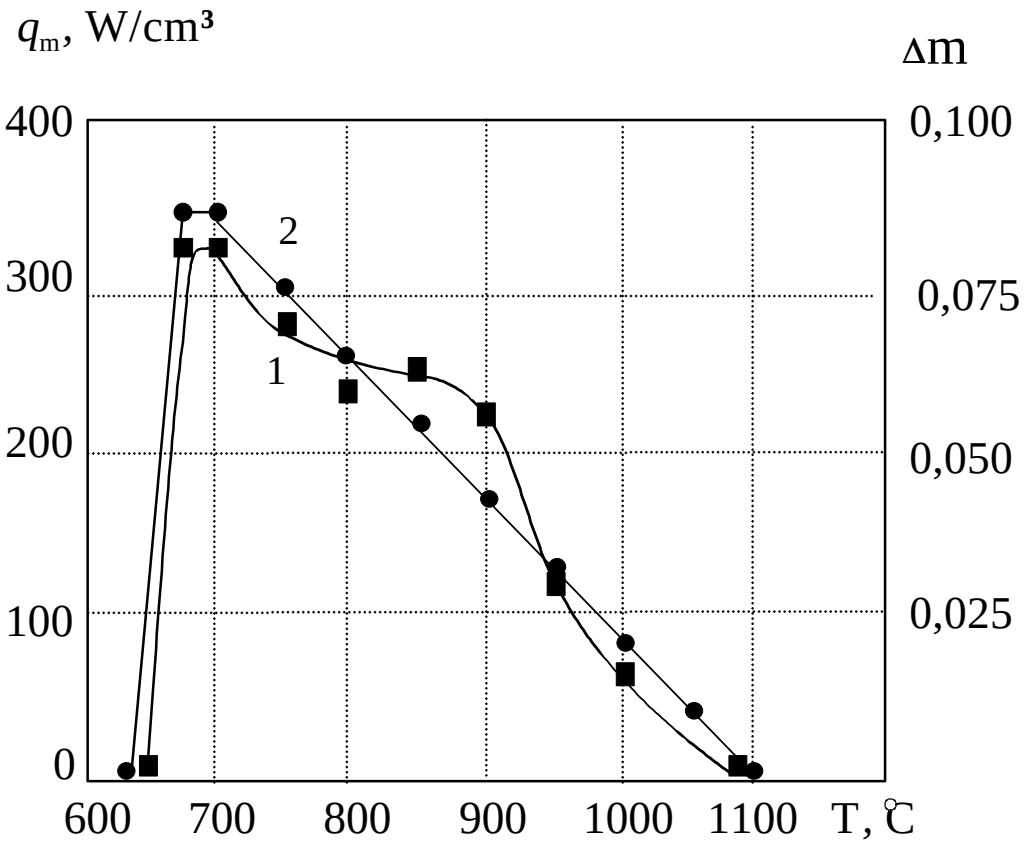

Fig. 7. The theoretical Δm as a function of T (1) and rate of heat release vs. temperature (2).

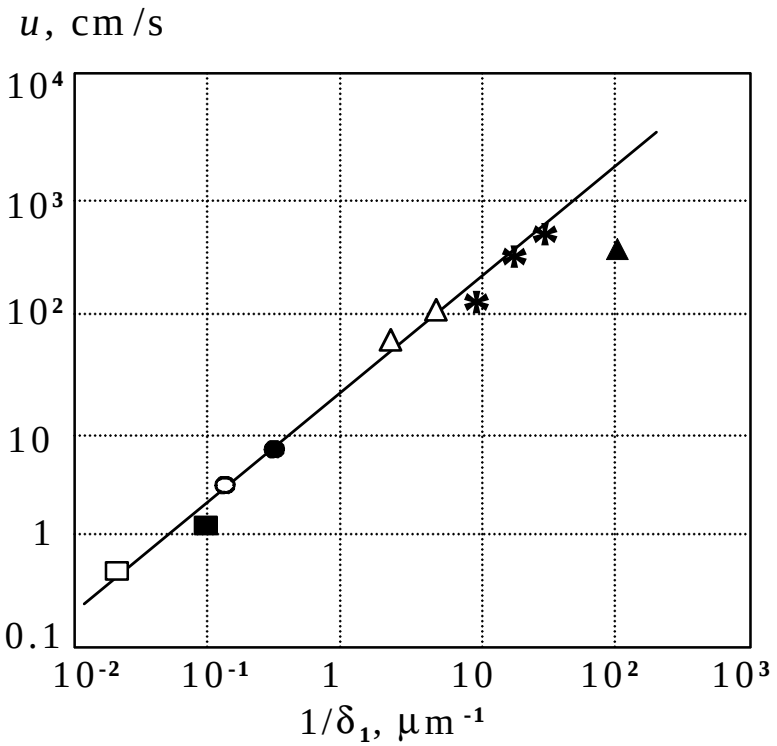

Fig. 8. Combustion velocity vs. Al layer thickness.

■ - [Maslov *et al.*,1976];
○ - [Lebrat *et al.*, 1992];
△ - [Dyer *et al.*, 1995];
□ [Present study];
● - [Naiborodenko *et al.*,1975];
▲ - [Ma *et al.*, 1990];
✱ - [Weihs *et al.*, 1997].